






Comparison of Keratometric Changes After Ab Interno Gel Stent Implantation, Glaucoma Drainage Devices and Trabeculectomy

Kenan Bachour ^{1,2}, Dominique Geoffrion ¹⁻³, Guillaume A Mullie ^{1,4,5}, Younes Agoumi ^{1,2},
Georges M Durr ^{1,2}

¹Department of Ophthalmology, Université de Montréal, Montreal, Canada; ²Department of Ophthalmology, Centre Hospitalier de l'Université de Montréal, Montreal, Quebec, Canada; ³Faculty of Medicine, McGill University, Montreal, Quebec, Canada; ⁴Department of Ophthalmology and Visual Sciences, McGill University, Montreal, Quebec, Canada; ⁵St. Mary's Hospital, Montreal, Quebec, Canada

Correspondence: Kenan Bachour, Department of Ophthalmology, Université de Montréal, 2900 Bd Édouard-Montpetit, Montréal, Montreal, Quebec, QC H3T 1J4, Canada, Tel +1 514 677-9601, Email kenan.bachour@umontreal.ca; Georges M Durr, Department of Ophthalmology, Université de Montréal, 1051 Rue Sanguinet, Montreal, Quebec, H2X 3E4, Canada, Email georgesdurr@gmail.com

Purpose: To compare postoperative keratometric changes and surgically induced astigmatism (SIA) after Ab Interno Gel Stent Implantation (XEN), glaucoma drainage device (GDD), and trabeculectomy (TRAB). GDDs included Ahmed glaucoma valve (AGV) and Baerveldt glaucoma implant (BGI).

Design: Prospective, interventional, longitudinal study.

Participants and Methods: Fifty-one eyes with glaucoma undergoing glaucoma filtering surgery were recruited between November 2020 and May 2023. The groups consisted of 19 XEN implants (37%), 21 GDDs (41%) (2 AGVs, 19 BGIs), and 11 trabeculectomies (22%). Primary outcomes were SIA at 12 months postoperatively, measured by Pentacam (Scheimpflug imaging) and OPD-scan (topography). The arithmetic mean of SIA (M-SIA) and the centroid of SIA (C-SIA) were determined using vector analysis. Secondary outcomes included BCVA, IOP, number of meds, and complications.

Results: At 12 months, C-SIA measured by tomography was similar across all groups (0.3 ± 1.0 D for XENs and GDDs and 0.4 ± 1.0 D for TRAB). Topography measurements demonstrated a C-SIA of 0.2 ± 0.9 D for XENs, 0.1 ± 0.9 D for GDD, and 0.6 ± 1.7 D for TRAB. TRAB showed a trend towards a higher proportion of eyes with >1 D of astigmatism (73%) compared to the XEN (27%) and GDD groups (48%, $p = 0.159$).

Conclusion: SIA was similar across groups when measured by tomography, while topography measurements indicated a trend towards more SIA with TRAB. Mean cylinder values at 12 months were higher in the TRAB group.

Keywords: glaucoma, surgically induced astigmatism, cornea, keratometric changes

Introduction

Following glaucoma surgery, patients can often experience a decrease in visual acuity due to multiple causes, including changes in the cornea's optical properties.^{1,2} Traditional filtering surgeries, such as trabeculectomy (TRAB) and glaucoma drainage devices (GDD), including the Baerveldt glaucoma implant (BGI, Johnson & Johnson Vision Care Inc., Jacksonville, FL) and the Ahmed glaucoma valve (AGV, New World Medical, Rancho Cucamonga, California), are often effective in reducing IOP. However, inconsistent visual recovery caused by changes in corneal curvature and postoperative scarring, along with a significant risk of complications, have driven interest in exploring alternative glaucoma procedures.² Surgically induced astigmatism (SIA) can impact postoperative visual acuity and patient satisfaction, even when intraocular pressure is adequately controlled. Therefore, understanding the magnitude and pattern of SIA has important clinical implications for visual rehabilitation and patient outcomes following glaucoma surgery.³

In recent years, less invasive surgeries known as ‘minimally invasive glaucoma surgery’ (MIGS) have gained popularity in the surgical management of glaucoma.⁴ Among these, the XEN Gel Stent (Allergan Inc., Irvine, California, USA) is a 6-mm flexible gelatin-based implant designed to create a tunnel between the anterior chamber and the subconjunctival space outside the eye, facilitating aqueous humor drainage.⁵ Compared to other glaucoma filtering surgeries, the XEN is implanted without opening the conjunctiva, and the implant tip is located further from the limbus, potentially causing less keratometric changes than other filtering surgeries.

Despite being performed for decades, limited research has focused on corneal astigmatism following glaucoma surgery.^{6–13} To our knowledge, no study has yet compared the keratometric changes after XEN, GDD, and TRAB. Therefore, the aim of this study was to evaluate the postoperative corneal astigmatism induced by the implantation of the XEN device compared to that induced by traditional filtering surgeries (GDD and TRAB).

Methods

Study Design

This study is a prospective interventional comparative study involving patients undergoing standalone glaucoma filtering surgery at the Centre Hospitalier de l’Université de Montréal (CHUM) between November 2020 and May 2023 by two surgeons (GD and YA). This study received approval from the Ethics Committee (20.240) of the Centre Hospitalier de l’Université de Montréal (CHUM) and adhered to the tenets of the Declaration of Helsinki.

Inclusion and Exclusion Criteria

Adults with uncontrolled glaucoma under maximal tolerated medical therapy, who were candidates for standalone glaucoma filtering surgery (XEN, GDD, or trabeculectomy¹⁴), were screened for inclusion. Selected participants provided informed consent. Exclusion criteria included glaucoma surgery combined with any other surgical procedure, eyes with corneal diseases. Any patient who experienced significant postoperative complications necessitating additional surgical interventions was excluded from the analysis as of the time of the complication or subsequent surgery.

Data Collection

Data collection was anonymized and performed using Microsoft Excel (v.16.86 2024 (Redmond, Washington, USA)). Preoperative data were obtained, which included: age, sex, medical and ocular history, best corrected visual acuity (BCVA), IOP, number of glaucoma drops (meds), keratometric and autorefractometry measurements via specular reflection corneal topography using Optical Path Difference Scanning System (OPD-Scan III; NIDEK Inc, Tokyo, Japan), corneal topography using Scheimpflug imaging (Pentacam imaging; Oculus Optikgeräte GmbH, Wetzlar, Germany), Humphrey 24–2 (Swedish Interactive Threshold Algorithm (SITA)-Fast) visual fields (VF) data (visual field index (VFI), mean deviation (MD)), Simulated keratometry (SimK) values were used for topography measurements, while anterior corneal power was utilized for tomography assessments.

Postoperative data collected at 2, 6, and 12 months included the following: BCVA, IOP, meds, autorefractometry, keratometric measurements via OPD-Scan and Pentacam imaging. Postoperative complications were noted at all visits (eg hyphema, IOP spikes, hypotony, etc.), as well as interventions (eg needling, anterior chamber reformation, etc.).

Outcome Measurements

The primary outcome was the SIA measured at 2, 6 and 12 months postoperatively using OPD-scan and Scheimpflug imaging. Secondary outcomes included BCVA, IOP, number of meds, and complications.

Assessment of SIA

SIA was calculated based on the vector analysis algorithm, as previously described by Alpíns et al and Holladay et al^{15,16} The arithmetic mean of SIA (M-SIA), which is the mean of only the magnitude of SIA, and the centroid of SIA (C-SIA), which is the mean SIA vector considering magnitude and direction, were determined. The magnitudes of SIA are expressed as centroid or mean \pm standard deviation. Double-angled plots of the corneal SIA were generated using the

“Corneal SIA Tool V.1.0.0” Excel spreadsheet, available on the American Society of Cataract and Refractive Surgery website.^{17,18} When evaluating the axis of astigmatism, the side of the operated eye (right or left) was taken into account ensuring that axis measurements were analyzed consistently.

Topographic analysis was performed using the OPD-Scan III (Nidek Co., Japan), which provides anterior corneal surface measurements and wavefront data. Tomographic imaging was conducted with the Pentacam (Oculus, Germany), which uses a rotating Scheimpflug camera to capture both anterior and posterior corneal surfaces. The use of both modalities ensured an accurate assessment of SIA by combining complementary data sources.¹⁹

Sample Size Determination

The sample size was determined using the G*Power software (Version 3.1.9.6, Heinrich-Heine-Universität Düsseldorf, Düsseldorf, Germany) with a one-way ANOVA for multiple groups. To achieve 80% power, we aimed for a sample size adjusted for a 10% loss to follow-up, which resulted in a required total of 57 participants, or 19 per group. However, the recruitment ceased from April 2020 to April 2021 due to COVID-19 pandemic-related delays and insufficient resources to continue. As a result, the target number of participants could not be obtained in all groups.

Data Analysis

Statistical analysis was performed using SPSS (v29.0, IBM Corp). A p -value ≤ 0.05 was considered significant. Normality was assessed with the Shapiro–Wilk test. Categorical variables were compared using the Chi-square test, and continuous variables with the Student’s t -test (normal distribution) or Mann–Whitney U -test (non-normal). The Wilcoxon test was used for paired samples, and the Kruskal–Wallis test compared three groups.

Surgical Procedures

The same surgical techniques were used by both surgeons in this study, as described below.

XEN Implant

A temporal paracentesis was made followed by an inferotemporal incision with a 2.2 mm keratome. The injector with the implant was introduced into the anterior chamber through the inferotemporal incision and was then advanced into the angle of the superonasal quadrant until 3 mm posterior to the limbus, where the XEN implant was then released into the subconjunctival space. The implantation was followed by a subconjunctival injection of 0.1 cc of 0.04% Mitomycin C (MMC) over the area of XEN insertion.

BGI and AGV

A conjunctival peritomy was performed 6 mm from the limbus in the superotemporal quadrant or with relaxing incisions as per surgeon preference. Sub-Tenon’s dissection created space for the implant. The tube was inserted under (BGI) or between (AGV) the rectus muscles, fixed 10 mm from the limbus, and cut obliquely to leave 2 mm in the anterior chamber. For BGI, a 7–0 Vicryl ligature occluded the tube. A 1 mm paracentesis allowed viscoelastic/BSS injection, and a 23-gauge syringe created the path for the tube, which was covered with a 2×3 mm scleral graft. A running suture was then used to close the conjunctiva and Tenon’s capsule over the scleral graft. The conjunctiva and Tenon’s capsule were closed using running or wing and interrupted sutures.

Trabeculectomy

A 4 mm fornix-based conjunctival flap was created at the limbus, releasing Tenon’s capsule. A 3.0×2.0 mm partial-thickness scleral flap was made, and a 1 mm temporal paracentesis allowed viscoelastic injection. A 2.2 mm keratome created anterior chamber access, followed by a scleral punch for the sclerotomy. The scleral flap was closed with 10–0 nylon sutures, and flow was verified by injecting BSS. The sutures were buried, a bleb confirmed, and the conjunctiva and Tenon’s capsule were closed with two winged 9–0 nylon sutures.

Standard postoperative medications were used including a steroid and nonsteroidal anti-inflammatory drop, a topical antibiotic drop. The addition of glaucoma eyedrops and any further glaucoma procedure was done at the discretion of the surgeons.

Results

Demographics

Fifty-one eyes of 50 patients with glaucoma were included in this study. The number of eyes per group was as follows: 19 in the XEN group (37%), 21 in the GDD group (41%), and 11 in the TRAB group (22%). Of the 21 eyes in the GDD group, 19 eyes had BGI and two eyes had AGV. Demographics and baseline characteristics of participants are summarized in [Table 1](#). Mean follow up period was 53 ± 8 weeks. Previous cataract surgery with intraocular lens implantation was done in 86% of eyes ($n = 43$). For the proportion of glaucoma subtypes per group, refer to [Supplemental Table 1](#).

Visual Changes

[Figure 1](#) displays BCVA changes across visits. After surgery, visual acuity did not vary significantly compared to baseline at any of the measured postoperative time points for GDD and TRAB eyes ([Table 2](#)). For XENs, BCVA was worse at 12 months ($p = 0.049$) when compared to baseline.

Keratorefractive Changes

[Table 3](#) shows the spherical shift one year after surgery. A hyperopic shift was seen in only 5 eyes (29%) following XEN implantation, compared to 12 eyes (63%) after GDD and 6 eyes (60%) after TRAB ($p = 0.317$). For mean spherical changes over time, refer to [Supplemental Table 2](#).

[Figure 2](#) shows a clustered bar chart of corneal astigmatism before and after surgery. Preoperatively, the proportions of eyes within all subcategories of astigmatism (0–0.50; 0.51–1.00; >1.00D) were similar in all three groups ($p = 0.980$). [Figure 3](#) shows the changes in cylinder power before and after surgery as measured by OPD-scan and Pentacam imaging. At the 12-month follow-up, the mean cylinder remained similar to baseline for the XEN (1.0 ± 0.6 D, $p = 0.603$) and GDD (1.2 ± 0.8 D, $p = 0.068$) groups, but increased to 1.6 ± 0.9 D in the TRAB group ($p = 0.008$). The TRAB group showed a significant increase in cylinder at all postoperative visits, but there was no statistically significant difference in cylinder between all three groups at 12 months ($p = 0.154$). For detailed changes in cylinder power and axis, refer to [Supplemental Table 3](#).

[Figure 4](#) presents double-angled plots of corneal SIA across all visits for the three groups, measured by topography (4A) and tomography (4B). At the 2-month mark, the highest C-SIA was consistently observed in the TRAB group: 0.7 ± 1.3 D on OPD-scan and 0.7 ± 1.0 D on Pentacam. By the final visit, the C-SIA had decreased in all groups, but remained higher in the TRAB eyes (0.6 ± 1.7 D) as compared to XENs (0.2 ± 0.9 D) and GDDs (0.1 ± 0.9 D) as per OPD-scan data. Pentacam

Table 1 Baseline Characteristics

Variable	XEN	GDD	TRAB	p-Value
Age (years)	77 ± 8	71 ± 10	65 ± 11	0.018
Female	11 (58)	11 (52)	4 (36)	0.517
Previous cataract surgery	16 (84)	21 (100)	7 (64)	0.017
Preoperative IOP (mmHg)	25 ± 9	24 ± 6	21 ± 6	0.345
Preoperative maximum IOP (mmHg)	32 ± 9	33 ± 9	26 ± 6	0.104
Preoperative meds	3.7 ± 0.7	3.3 ± 1.0	3.2 ± 1.1	0.386
OCAI	5 (26)	5 (24)	1 (9)	0.515
BCVA (logMAR)	0.13 ± 0.14	0.32 ± 0.40	0.22 ± 0.21	0.446
CCT (μm)	526 ± 65	532 ± 41	534 ± 43	0.999
Spherical Equivalent (D)	-0.4 ± 0.8	-0.8 ± 0.8	-2.1 ± 4.1	0.244

Notes: The p-value was calculated using the Kruskal–Wallis test for continuous variables and the Chi-square test for categorical variables. Significant p-values are highlighted in bold. Categorical variables are presented as n(%); and continuous variables as mean \pm SD.

Abbreviations: BCVA, best-corrected visual acuity; CCT, central corneal thickness; GDD, glaucoma drainage device; IOP, intraocular pressure; logMAR, Logarithm Of The Minimum Angle Of Resolution; Meds, number of glaucoma medication; OCAI, oral carbonic anhydrase inhibitor; SD, standard deviation; TRAB, trabeculectomy; XEN, XEN microstent implant.

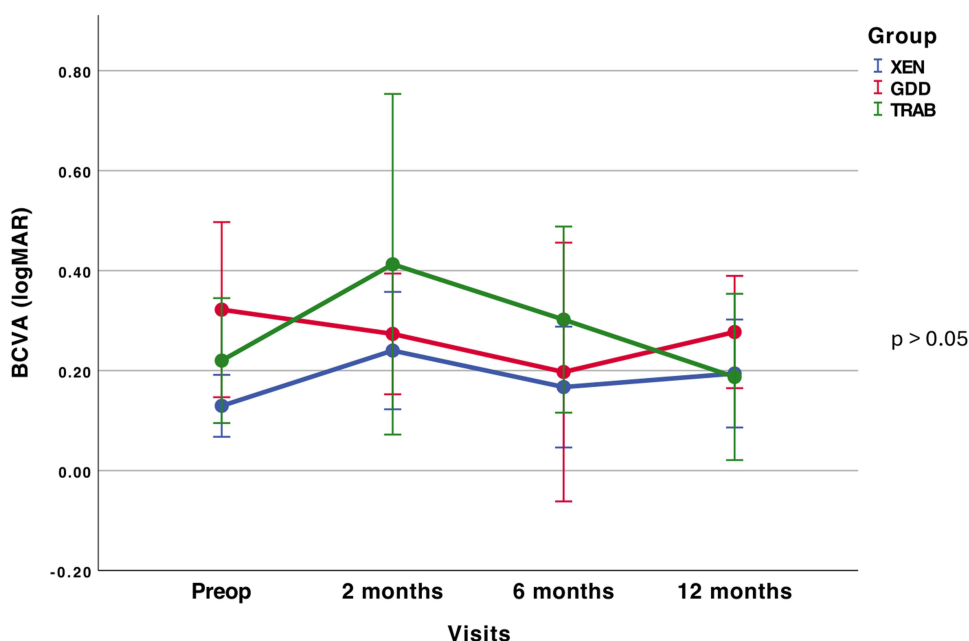


Figure 1 Mean BCVA variation across visits. The dots represent the mean value, and the bars show the standard error of the mean. The p-value was calculated using the Kruskal–Wallis test for intergroup comparisons.

Abbreviations: BCVA, best-corrected visual acuity; GDD, glaucoma drainage device; Preop, preoperative; TRAB, trabeculectomy; XEN, XEN microstent implant.

mirrored these trends, with final C-SIA remaining slightly higher in the TRAB group (0.4 ± 1.0 D). Due to the vectorial nature of C-SIA, no p-value could be generated. For detailed changes in C-SIA across visits, refer to [Supplemental Table 4](#).

For the OPD measurements, the initial 2-month postoperative M-SIA readings were highest across all groups: 0.9 ± 0.7 D for XEN, 1.3 ± 1.1 D for GDD and 1.3 ± 0.7 D for TRAB ($p = 0.263$). By 12 months, SIA had decreased to 0.8 ± 0.5 D for XEN, 0.8 ± 0.5 D for GDD, but remained high after TRAB (1.4 ± 1.9 D). Pentacam imaging results were slightly different, showing similar M-SIA for all groups at 12 months: 0.9 ± 0.5 D for both XEN and TRAB, and 0.8 ± 0.6 D for GDD ($p = 0.721$). For detailed changes in M-SIA across visits, refer to [Supplemental Table 5](#).

Table 2 BCVA Changes Across Visits

Variable	Visit	XEN	p-Value	GDD	p-Value	TRAB	p-Value	p-Value Intergroup Comparison
BCVA (logMAR)	Baseline	0.13 ± 0.14	-	0.32 ± 0.40	-	0.22 ± 0.21	-	0.446
	2 months	0.22 ± 0.25	0.056	0.27 ± 0.28	0.267	0.41 ± 0.56	0.173	0.669
	6 months	0.17 ± 0.256	0.355	0.33 ± 0.33	1.000	0.30 ± 0.29	0.293	0.194
	12 months	0.20 ± 0.24	0.049	0.28 ± 0.26	0.831	0.19 ± 0.28	0.351	0.384

Notes: Data presented as mean ± SD. The p-value was calculated using the Wilcoxon test for intragroup comparisons (preoperative to postoperative values) and the Kruskal–Wallis test for intergroup comparisons. Significant p-values are highlighted in bold.

Abbreviations: BCVA, best corrected visual acuity; GDD, glaucoma drainage device; MD, mean deviation; SD, standard deviation; TRAB, trabeculectomy; XEN, XEN microstent implant.

Table 3 Spherical Shift at 12 months

Variable	XEN	GDD	TRAB	p-Value
Hyperopic shift	5 (29)	12 (63)	6 (60)	0.317
Myopic shift	8 (47)	5 (26)	3 (30)	0.306
Neutral	4 (24)	2 (11)	1 (10)	0.086

Notes: The p-value was calculated using the Chi-square test. Data presented as n (%).

Abbreviations: GDD, glaucoma drainage device; TRAB, trabeculectomy; XEN, XEN microstent implant.

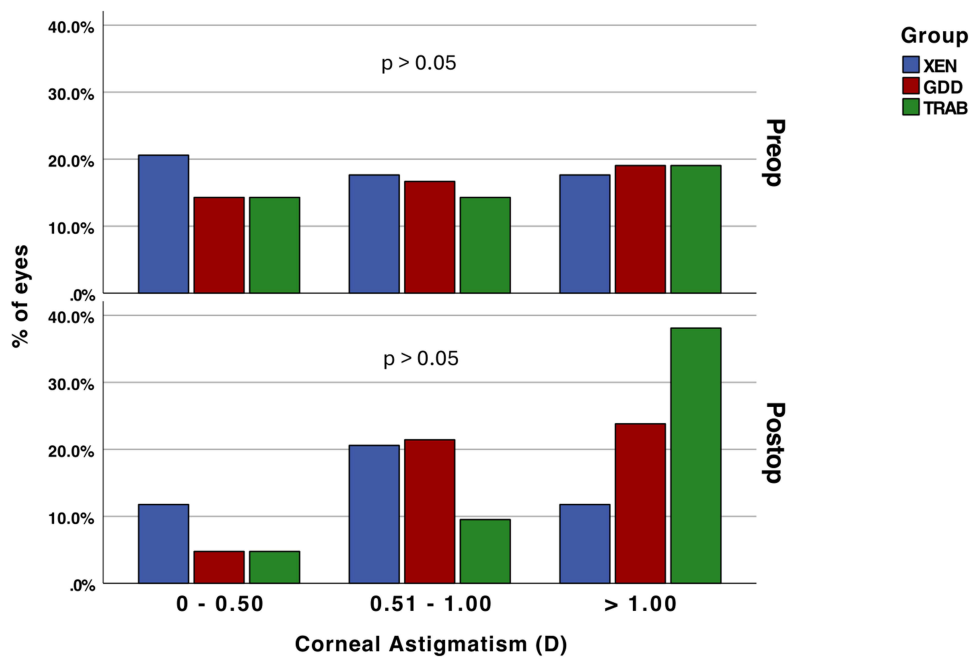


Figure 2 Clustered bar of the proportion of corneal astigmatism preoperatively and at 12 months. The p-value was calculated using the Chi-square test. **Abbreviations:** D, diopter; GDD, glaucoma drainage device; TRAB, trabeculectomy; XEN, XEN microstent implant.

For both the XEN and GDD groups, initial SIA axes differed depending on the measurement device. On Pentacam imaging measurements, the XEN group’s C-SIA demonstrated predominantly against-the-rule (ATR) and oblique (OBL) axes over 12 months, ranging from 115 ± 28 degrees to 157 ± 21 degrees. However, at 12 months, both measurements methods showed an ATR axis (177 to 179 degrees) for GDD. The TRAB group showed an initial WTR shift (84 ± 13 degrees), followed by a mild ATR shift (68 ± 25 degrees) at 12 months on OPD-scan. However, the axis remained WTR on Pentacam, ranging from 77 ± 15 degrees to 89 ± 11 degrees.

Glaucoma Outcomes

In all three groups, there was a significant reduction in IOP and the mean number of meds at all visits ($p < 0.015$). The TRAB group had significantly less meds than XENs and GDDs at 12 months: 0.6 ± 1.0 meds compared to 2.3 ± 1.2 for GDD ($p = 0.002$) and 1.6 ± 1.4 for XEN ($p = 0.147$) at 12 months. For additional details on the mean IOP and number of glaucoma meds per visit, refer to [Supplemental Table 6](#).

Table 4 shows postoperative complications. The two most common complications were transient increases in IOP (>21 mmHg, $n = 16$) and transient hypotony ($n = 13$). Two bleb leaks were reported in the TRAB group, presenting on average 1 week after surgery. Another bleb leak was noted in the XEN group, initially requiring secondary wound closure, and later an internal revision of the microstent due to exposure of the implant.

Discussion

The focus of this study was to compare the SIA after XEN surgery, GDD implantation and TRAB. To our knowledge, no prior study has directly compared these three groups. Our study demonstrated measurable postoperative astigmatic changes in all three groups but did not show any significant intergroup difference although there was a trend for higher SIA in the TRAB group on topography measurements.

Existing studies have already reported that it is common for patients undergoing glaucoma surgery to have a period of reduced visual acuity in the early postoperative period.²⁰ Reasons could be an IOP-, bleb- or suture-associated deformation of the cornea in the early postoperative phase. SIA has been hypothesized to contribute to this reduction in visual acuity. Several factors, including the location and surgical technique, can influence corneal astigmatism change.

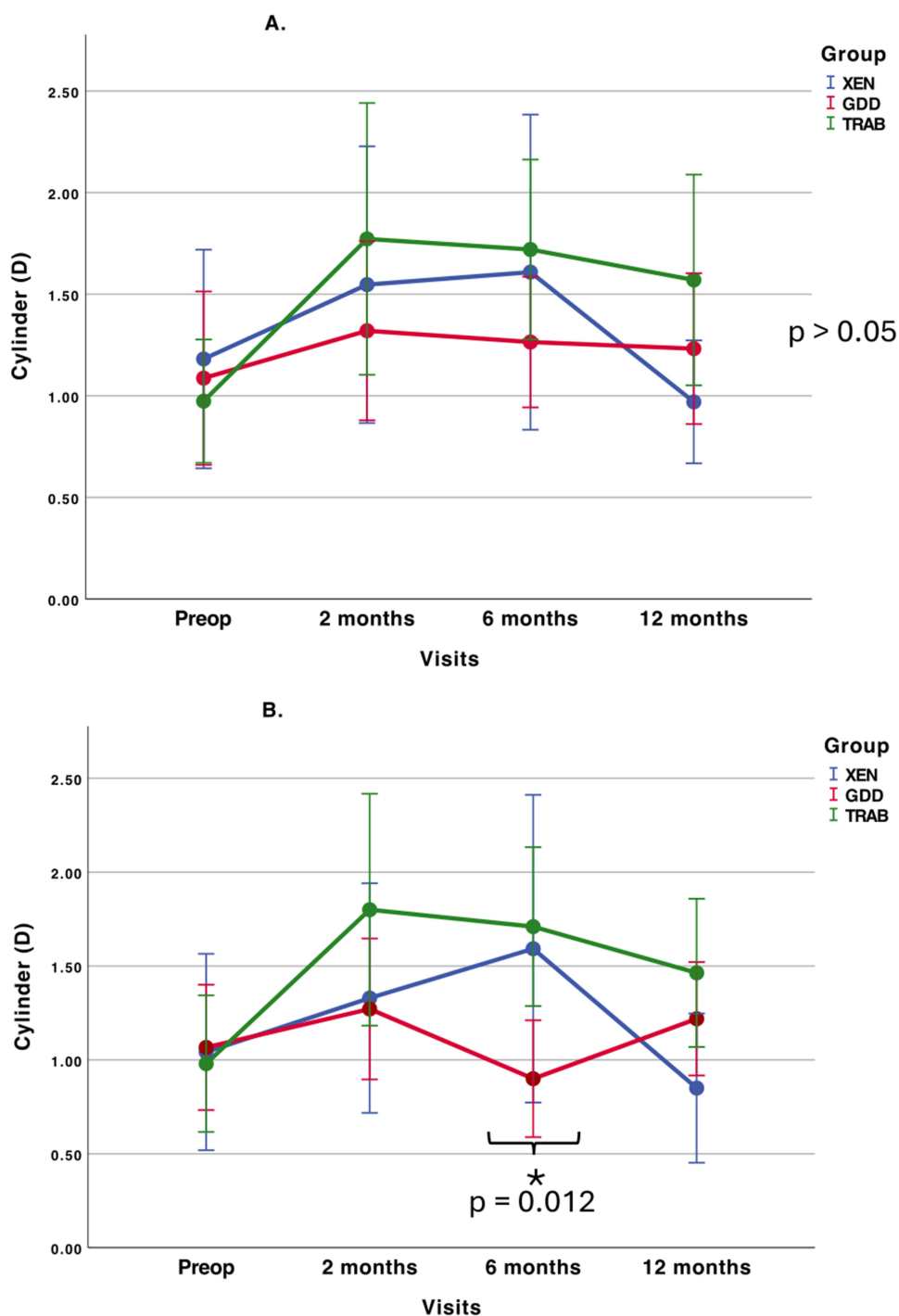


Figure 3 Cylinder power measured by topography and tomography. (A) Cylinder power changes measured by OPD-scan. (B) Cylinder power changes measured by Pentacam. The dots represent the mean value, and the bars show the standard error of the mean. The p-value was calculated using the Kruskal–Wallis test for intergroup comparisons. Significant p-values are marked with an asterisk.

Abbreviations: D, diopter; GDD, glaucoma drainage device; OPD, optical path difference scanning system; Pentacam, Pentacam imaging; Preop, preoperative; TRAB, trabeculectomy; XEN, XEN microstent implant.

In our study, BCVA did not significantly vary from baseline at all postoperative points, except unexpectedly for the XEN group, which showed a decrease in visual acuity at 12 months. We were unable to identify any specific explanation for this decrease. It is possible that this finding may simply be related to disease progression. However, as the p-value barely reached statistical significance, this observation may not be indicative of a true clinical effect.

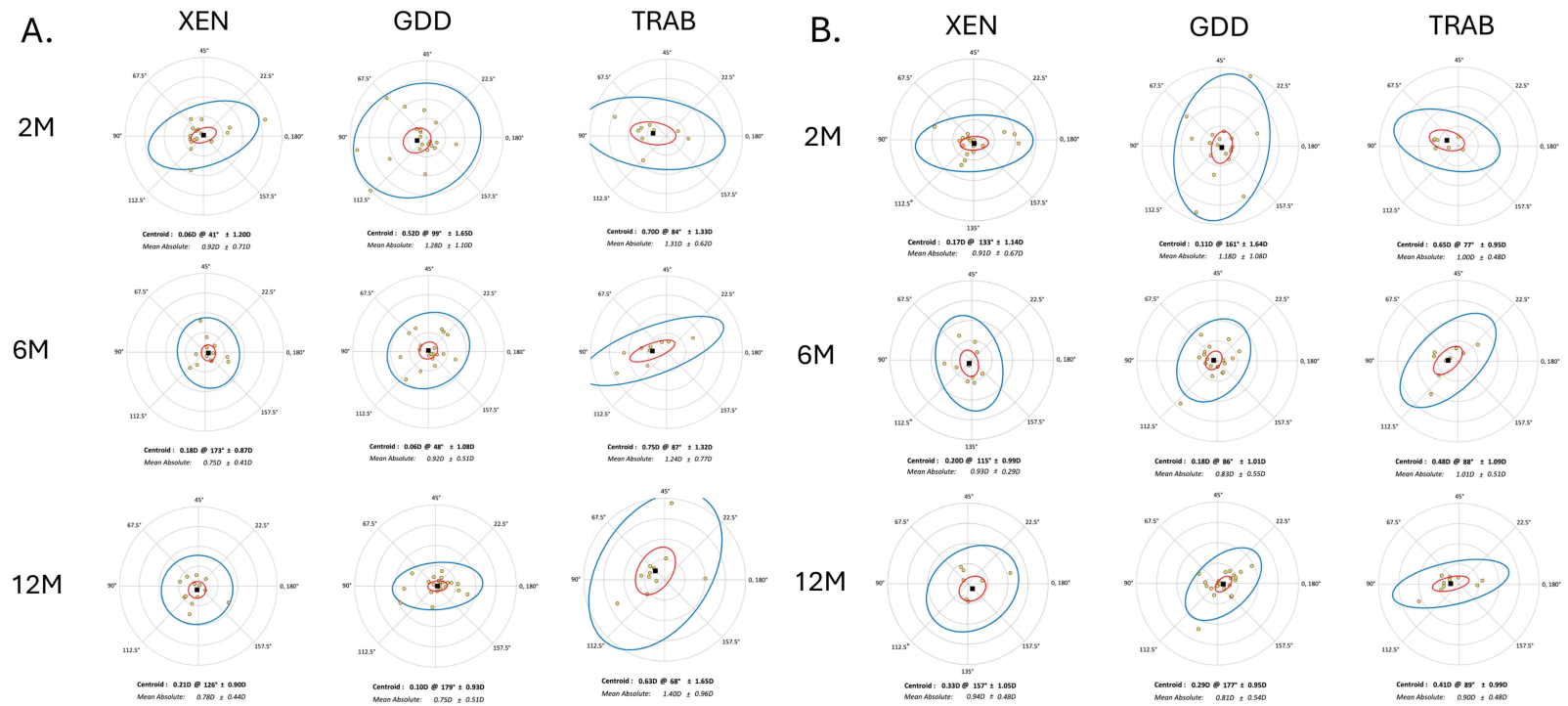


Figure 4 Double-angled plots of the SIA at 2, 6, and 12 months measured by topography (**A**) and tomography (**B**). Black square and yellow dots indicate the centroid SIA and the mean SIA of each eye, respectively. Standard deviations (SD), and 95% confidence ellipses of the centroid (red) and dataset (blue) are displayed. Each ring represents 1D.

Abbreviations: D, diopters; GDD, glaucoma drainage device; M, months; TRAB, trabeculectomy; XEN, XEN microstent implant.

Table 4 Complications

Complications	XEN	GDD	TRAB	p-Value
Increased IOP (>21 mmHg)	4 (21)	9 (43)	3 (27)	0.315
Transient hypotony (<6mmHg for <3 months)	3 (16)	7 (33)	3 (27)	0.440
Chronic hypotony (<6mmHg for >3 months)	0	1 (5)	0	0.483
Choroidal detachment	1 (5)	1 (5)	0	0.749
Hyphema	0	2 (10)	0	0.226
Bleb leak (Seidel +)	1 (5) ^a	0	2 (18)	0.120
Tube exposure	1 (5) ^a	0	0	0.424
Corneal abrasion during surgery	0	1 (5)	2 (18)	0.120
Corneal edema	0	1 (5)	0	0.483
Cystoid macular edema	1 (5)	4 (19)	0	0.160

Notes: The p-value was calculated using the Chi-square test. ^aOne eye in the XEN group had a bleb leak, necessitating an internal review of the microshunt due to tube exposure.

Abbreviations: GDD, glaucoma drainage device; IOP, intraocular pressure; TRAB, trabeculectomy; XEN, XEN microstent implant.

Most studies that evaluated keratometric changes after TRAB have revealed significant induced WTR astigmatism, which was in some cases followed by an ATR shift, which tends to resolve within 1 year.^{1,6} Hugkulstone et al were the first to investigate SIA as a possible cause for a decrease in the visual acuity after TRAB.²¹ Studies have also shown that using MMC in TRAB is associated with longer-lasting astigmatic changes.²² Our findings are consistent with previous studies, as our TRAB group showed a C-SIA of 0.7 ± 1.3 D accompanied by a WTR shift (84 ± 13 degrees) at 2 months which was then followed by an ATR shift (0.6 ± 1.7 D at 68 ± 25 degrees) at 12 months. When looking at the change in cylinder over visits, the TRAB group showed a trend towards an increase in astigmatism at 12 months when compared to baseline, as recorded by both Pentacam and OPD-scan.

Limited data exists on the refractive outcomes following GDD surgery. Kousslavio et al showed that astigmatism and corneal keratometry remained unchanged after 1 year following BGV or Molteno valve (Molteno Ophthalmic Ltd., Dunedin, New Zealand) implantation.⁹ Miraftebi et al also reported that AGV implantation had no significant effect on the refractive error and corneal curvature.¹⁰ These findings align with our study, in which we found that GDD did not induce any significant SIA, with only 0.1D of C-SIA on OPD-scan and 0.4D on Pentacam. The mean cylinder did not vary postoperatively (1.1 ± 1.0 at 12 months) when compared to baseline (1.2 ± 1.0 D, $p = 0.068$).

Some studies have started to report on keratometric changes after XEN surgery. Schlenker et al reported on the SIA after TRAB and XEN.²³ Forty-four percent and 17% of TRAB eyes, compared to 26% and 8% of XEN eyes had more than 0.5D and 1D of SIA, respectively. The authors hypothesized that this difference stems from the absence of sutures to close the conjunctiva in microstent procedures. However, astigmatism measurements in this study were not performed systematically and relied only on autorefractometry, and the authors acknowledged the need for more accurate measures as well as the need to take astigmatism axis into account. Similarly, we also found that TRAB eyes had a higher proportion of astigmatism >1D postoperatively (73%) when compared to the XEN group (27%). Another study by Bormann et al showed that the SIA was similar after TRAB and XEN implantation, with an average of 0.8D for both XEN and TRAB ($p = 0.57$).¹¹ Comparatively, at the one year follow-up visit, we observed a C-SIA of 0.3D after XEN and 0.6D after TRAB on OPD-scan, suggesting a higher trend of SIA for trabeculectomies.

Although the induction of postoperative astigmatism has not been explicitly ruled out for the new emerging MIGS procedures, it could be assumed that the minor surgical trauma, the absence of transscleral sutures, and the implant tip being located further from the limbus, resulting in a more posterior bleb, could result in a lower SIA after XEN compared to the traditional filtering surgeries.

Assessing astigmatic changes poses challenges related to its two components: the magnitude and axis of the cylinder. Methods have been developed to calculate SIA, including trigonometric equations by Jaffe and Clayman, as well as the polar method.^{24,25} While these approaches attempt to quantify the magnitude and orientation of SIA, they all face limitations due to the complex nature of astigmatism. To address these challenges, data is often combined using vector magnitude differences

to describe induced astigmatic changes.²⁴ A recent trend for analyzing and displaying SIA results utilizes a double-angled polar plot to describe the corneal change's magnitude and axis, which is the approach we have adopted.¹⁶

This study has several strengths. As mentioned, it is the first to compare the SIA after XEN, GDD and TRAB. Due to the prospective nature of the study, we minimized the likelihood of missing data during follow-up visits. To assess keratometric changes, we utilized two imaging modalities: topography with the OPD-scan and tomography with Pentacam imaging.

However, our study also presents some limitations. The small number of participants in the TRAB group may have affected the study's statistical power. As noted previously, no single method perfectly represents astigmatic changes. To address this, we employed the Alpins method, and we illustrated SIA using double-angled plots to describe the magnitude and axis of corneal changes. Finally, the number of AGV cases was too small to allow for comparisons of outcomes by tube type.

Conclusion

XEN and GDD may induce less SIA compared to TRAB when measured by OPD-scan, although Pentacam imaging showed similar SIA trends across all groups. Keratometric changes associated with emerging MIGS procedures remain under-studied. Future research with larger sample sizes is needed to comprehensively compare the refractive outcomes of these new MIGS procedures with traditional filtering surgeries.

Declaration of Generative AI in Scientific Writing

During the preparation of this work, the authors used ChatGPT (Version 4.0, OpenAI, 2024) in order to readability and language. After using this tool, the authors reviewed and edited the content as needed and take full responsibility for the content of the publication.

Acknowledgments

Preliminary results were presented at the American Society of Cataract and Refractive Surgery Annual Meeting 2022 and at the Canadian Ophthalmological Society Annual Meeting 2024.

This paper has been uploaded to the Université de Montréal's institutional repository as a thesis: [<https://umontreal.scholaris.ca/server/api/core/bitstreams/e09818b9-51da-4b2e-b500-97f555c40c41/content>].

Funding

This work was supported by Allergan/Abbvie Inc., Irvine, California, USA; and the University of Montreal Research Funds (FROUM).

Disclosure

Dr. GM Durr reports consultancy, research supports for and/or lecture fees from Alcon Laboratories Inc, Allergan Inc, Avisi Technologies Inc, Bausch and Lomb, Glaukos Corporation, Ivantis Inc, Johnson and Johnson, Latician Ophthalmics Inc, MicroSurgical Technology, Novartis Pharma AG, Santen Inc, Sight Sciences Inc. The other authors report no conflicts of interest in this work.

References

1. Chan HHL, Kong YXG. Glaucoma surgery and induced astigmatism: a systematic review. *Eye Vis.* 2017;4(1):27. doi:10.1186/s40662-017-0090-x
2. Lim R. The surgical management of glaucoma: a review. *Clin Exp Ophthalmol.* 2022;50(2):213–231. doi:10.1111/ceo.14028
3. Schallhorn SC, Hettinger KA, Pelouskova M, et al. Effect of residual astigmatism on uncorrected visual acuity and patient satisfaction in pseudophakic patients. *J Cataract Refract Surg.* 2021;47(8):991–998. doi:10.1097/j.jcrs.0000000000000560
4. Saheb H, Ahmed II. Micro-invasive glaucoma surgery: current perspectives and future directions. *Curr Opin Ophthalmol.* 2012;23(2):96–104. doi:10.1097/ICU.0b013e32834ff1e7
5. Chatzara A, Chronopoulou I, Theodossiadis G, Theodossiadis P, Chatziralli I. XEN Implant for Glaucoma Treatment: a Review of the Literature. *Semin Ophthalmol.* 2019;34(2):93–97. doi:10.1080/08820538.2019.1581820
6. Pakravan M, Alvani A, Esfandiari H, Ghahari E, Yaseri M. Post-trabeculectomy ocular biometric changes. *Clin Exp Optom.* 2017;100(2):128–132. doi:10.1111/cxo.12477

7. Kim GA, Lee SH, Lee SY, et al. Surgically induced astigmatism following trabeculectomy. *Eye*. 2018;32(7):1265–1270. doi:10.1038/s41433-018-0072-9
8. Delbeke H, Stalmans I, Vandewalle E, Zeyen T. The Effect of Trabeculectomy on Astigmatism. *J Glaucoma*. 2016;25(4):e308–12. doi:10.1097/IJG.0000000000000236
9. Koivusalo R, Valimaki J. Effect of glaucoma drainage implant surgery on corneal topography: a prospective study. *Acta Ophthalmol*. 2020;98(3):305–309. doi:10.1111/aos.14247
10. Mirafzabi A, Lotfi M, Nilforushan N, Abdolalizadeh P, Jafari S. Ocular biometric changes after Ahmed glaucoma valve implantation. *Eur J Ophthalmol*. 2021;31(1):120–124. doi:10.1177/1120672119889528
11. Bormann C, Busch C, Rehak M, et al. Refractive Changes after Glaucoma Surgery-A Comparison between Trabeculectomy and XEN Microstent Implantation. *Life*. 2022;12(11). doi:10.3390/life12111889.
12. Schlenker MB, Gulamhusein H, Conrad-Hengerer I, et al. Standalone Ab Interno Gelatin Stent versus Trabeculectomy: postoperative Interventions, Visual Outcomes, and Visits. *Ophthalmol Glaucoma*. 2018;1(3):189–196. doi:10.1016/j.ogla.2018.10.003
13. Tatti F, Tronci C, Lixi F, et al. No Changes in Keratometry Readings and Anterior Chamber Depth after XEN Gel Implantation in Patients with Glaucoma. *J Clin Med*. 2024;13(9):2537. doi:10.3390/jcm13092537
14. Kirwan JF, Lockwood AJ, Shah P, et al. Trabeculectomy in the 21st century: a multicenter analysis. *Ophthalmology*. 2013;120(12):2532–2539. doi:10.1016/j.ophtha.2013.07.049
15. Alpíns N. Astigmatism analysis by the Alpíns method. *J Cataract Refract Surg*. 2001;27(1):31–49. doi:10.1016/S0886-3350(00)00798-7
16. Holladay JT, Moran JR, Kezirian GM. Analysis of aggregate surgically induced refractive change, prediction error, and intraocular astigmatism. *J Cataract Refract Surg*. 2001;27(1):61–79. doi:10.1016/S0886-3350(00)00796-3
17. ASCRS. Corneal SIA Tool. 2024. Available from: <https://ascrs.org/tools/corneal-sia-tool>. Accessed Sep 19, 2025
18. Koch DD, Wang L. Surgically Induced Astigmatism. *J Refract Surg*. 2015;31(8):565. doi:10.3928/1081597X-20150728-03
19. Ambrosio Jr R, Belin MW. Imaging of the cornea: topography vs tomography. *J Refract Surg*. 2010;26(11):847–849. doi:10.3928/1081597X-20101006-01
20. Cunliffe IA, Dapling RB, West J, Longstaff S. A prospective study examining the changes in factors that affect visual acuity following trabeculectomy. *Eye*. 1992;6(Pt 6):618–622. doi:10.1038/eye.1992.133
21. Hugkulstone CE. Changes in keratometry following trabeculectomy. *Br J Ophthalmol*. 1991;75(4):217–218. doi:10.1136/bjo.75.4.217
22. Hong YJ, Choe CM, Lee YG, Chung HS, Kim HK. The effect of mitomycin-C on postoperative corneal astigmatism in trabeculectomy and a triple procedure. *Ophthalmic Surg Lasers*. 1998;29(6):484–489. doi:10.3928/1542-8877-19980601-09
23. Schlenker MB, Gulamhusein H, Conrad-Hengerer I, et al. Efficacy, Safety, and Risk Factors for Failure of Standalone Ab Interno Gelatin Microstent Implantation versus Standalone Trabeculectomy. *Ophthalmology*. 2017;124(11):1579–1588. doi:10.1016/j.ophtha.2017.05.004
24. Holladay JT, Cravy TV, Koch DD. Calculating the surgically induced refractive change following ocular surgery. *J Cataract Refract Surg*. 1992;18(5):429–443. doi:10.1016/S0886-3350(13)80095-8
25. Naeser K. Assessment and statistics of surgically induced astigmatism. *Acta Ophthalmol*. 2008;86(1):5–28. doi:10.1111/j.1755-3768.2008.01234.x

Clinical Ophthalmology

Publish your work in this journal

Clinical Ophthalmology is an international, peer-reviewed journal covering all subspecialties within ophthalmology. Key topics include: Optometry; Visual science; Pharmacology and drug therapy in eye diseases; Basic Sciences; Primary and Secondary eye care; Patient Safety and Quality of Care Improvements. This journal is indexed on PubMed Central and CAS, and is the official journal of The Society of Clinical Ophthalmology (SCO). The manuscript management system is completely online and includes a very quick and fair peer-review system, which is all easy to use. Visit <http://www.dovepress.com/testimonials.php> to read real quotes from published authors.

Submit your manuscript here: <https://www.dovepress.com/clinical-ophthalmology-journal>

Dovepress
Taylor & Francis Group